

Long-time tails in angular momentum correlations

C. P. Lowe^{a)} and D. Frenkel

FOM Institute for Atomic and Molecular Physics, Kruislaan 407, 1098 SJ Amsterdam, The Netherlands

A. J. Masters

Department of Chemistry, University of Manchester, Manchester M13 9PL, England

(Received 23 February 1995; accepted 4 April 1995)

We compare computer simulation results for the angular velocity autocorrelation function (AVACF) of a colloidal particle with theoretical predictions. We consider both spherical and nonspherical particles in two and three dimensions. The theoretical prediction for the long-time decay of the AVACF in three dimensions is well known, here we also give the two-dimensional result, along with a sketch of how it was derived. For spherical particles we find excellent agreement between the simulations results and theoretical predictions in both two and three dimensions. We also find that the same expressions apply to the nonspherical particles *when* the particles have had time to undergo a significant angular displacement. This observation is again in agreement with theory. © 1995 American Institute of Physics.

I. INTRODUCTION

When Alder and Wainwright¹ computed the velocity autocorrelation function (VACF) of tagged particles in a hard sphere fluid they found, most surprisingly at the time, that the long-time decay was not exponential but algebraic. Up until then it was believed that at sufficiently long times, tagged particle motion could be regarded as a Markovian process—the particle would forget all about its past history and its VACF would decay exponentially. Alder and Wainwright were able to explain their observation in terms of the slow decay of the hydrodynamic fields set up by a moving object. In the intervening years more sophisticated theories have been developed following in the spirit of the original work. Mode coupling² and kinetic theories³ were developed to provide a theoretical framework for the description of these “long-time tails” in correlation functions. Slow algebraic decay was found not to be unique to the VACF but rather ubiquitous for time correlation functions. There is now a good measure of agreement between theory, experiment, and computer simulation. This is particularly true for the VACF where there is experimental evidence for long-time tails^{4–7} and computer simulation, performed by van der Hoef and Frenkel⁸ and by Ladd,⁹ shows excellent quantitative agreement with mode-coupling theory. The long-time algebraic decay of the stress–stress correlation function was also observed recently in a computer simulation and again found to be in agreement with mode-coupling theory.¹⁰

The correlation function we are interested in here is the *angular* velocity autocorrelation function (AVACF). If a particle has a rotational degree of freedom then we can define the AVACF as

$$\psi(t) = \langle \omega_z(0) \omega_z(t) \rangle, \quad (1)$$

where $\omega_z(t)$ is the angular velocity of the particle about the z

axis at time t . Ailawadi and co-workers^{11,12} were the first to predict the functional long-time form of the AVACF in d dimensions,

$$\psi(t) \sim (\nu t)^{-(d/2+1)}. \quad (2)$$

A precise prediction for the long-time decay of the AVACF for a spherical particle was derived by Hauge and Martin-Löf¹³ and by Chow.¹⁴ They found that, for a particle with moment of inertia I moving in a fluid with density ρ and kinematic viscosity ν , then

$$\psi(\infty) = \psi(0) \frac{I\pi}{\rho} (4\pi\nu t)^{-5/2}. \quad (3)$$

Equation (3) is only valid if the diffusion coefficient D for the object is negligible compared to the viscosity. If the diffusion coefficient is not negligible then it enters in essentially the same way as for the linear VACF,¹⁵ so the long-time tail in the AVACF takes the form

$$\psi(\infty) = \psi(0) \frac{I\pi}{\rho} [4\pi(\nu + D)t]^{-5/2}. \quad (4)$$

An analogous prediction for two dimensions has not, to our knowledge, been derived. One of our aims in this article is to present a theoretical expression for the AVACF in two dimensions and compare it with the results of computer simulation.

The first attempt to verify theoretical predictions for the decay of the AVACF was a study performed by Subramanian *et al.*¹⁶ of the rough hard sphere fluid. In view of the large statistical error in their numerical data, it required the eye of a believer to see any quantitative evidence for an algebraic decay of the angular velocity autocorrelation function. Simulations of an isolated colloidal particle performed by van der Hoef *et al.*¹⁷ were the first to demonstrate an algebraic form of the decay in two dimensions, although initially not with the expected exponent. More extensive simulations in two and three dimensions¹⁸ gave the expected power law decay. More recently, Ladd⁹ calculated the AVACF for a single colloidal sphere and compared it with the theoretical result ob-

^{a)}Current address: Computational Physics, Faculty of Applied Physics, Delft University of Technology, Lorentz Weg 1, 2628CJ Delft, The Netherlands.

tained by taking the inverse Laplace transform of the frequency dependent friction coefficient.¹³ He found agreement that was “essentially perfect over the whole time domain.”

There remains little to be said about the AVACF of a sphere, the theory has been tested and found to be highly satisfactory. For nonspherical objects the situation is not so clear, there are conflicting theoretical predictions. Masters and Keyes¹⁵ and Garisto and Kapral¹⁹ argue that Eq. (4) is valid for nonspherical objects whereas Hocquart and Hinch²⁰ and Cichocki and Felderhof²¹ suggest that the coefficient (not the exponent) of the long-time tail depends on the shape of the object. Preliminary simulations of a rotating nonspherical object suggested that the tail coefficient *was* shape dependent.¹⁸ Our second aim is to compute the long-time decay of the AVACF for nonspherical objects, to see if it is—or is not—dependent of particle shape.

The paper is structured as follows. First we give an outline of the theory used to derive the result for the tail coefficient in two dimensions and discuss under what circumstances the tail coefficient is predicted to be shape independent. Next we describe the model that we have used to simulate a colloidal particle and finally we compare the results of these simulations with theory.

II. OUTLINE OF THE THEORY

The theoretical derivation of the long time behavior of the AVACF for a nonspherical particle in two dimensions closely follows the three-dimensional approach given in Ref. 15. In order to avoid redeveloping the formalism contained in Ref. 15 we limit ourselves to a summary of the most important points. The derivation assumes that the particles interact via continuous pair potentials and then one analyses the memory function for the AVACF in terms of bilinear variables. Unlike the spherical particle case, these bilinear variables involve the orientation of the tagged particle. The analysis shows, however, that only the angularly isotropic components of these variables contribute to the asymptotic long-time behavior. The nonisotropic components decay exponentially due to reorientation of the particle. Thus, provided the rotational mobility is nonzero, one ends up with the result given in Eq. (4) in three dimensions, for a particle of arbitrary shape, mass, and size. In two dimensions one obtains

$$\psi(\infty) = \psi(0) \frac{I\pi}{\rho} [4\pi(\nu + D)t]^{-2}, \quad (5)$$

a result that is again valid for a tagged particle of any shape, size, or mass. In fact, the only way in which this expression varies between different tagged particles is due to the appearance of the translational diffusion constant, and very often this term is small compared to the kinematic viscosity of the fluid.

The simulation results quoted in this article are obtained from studying a Boltzmann lattice gas, not a continuous system interacting via continuous pair potentials, as assumed in the derivation. The analysis presented in Ref. 15 can, however, be readily generalized to deal with such a system and it would be surprising indeed if the final conclusions should

need to be altered. It should also be noted that the derivation sketched out above has assumed the existence of a zero-frequency shear viscosity and diffusion constant. In a “real” two-dimensional fluid this is not the case and Eq. (5) would have to be modified. In the simulation results quoted here, however, the center of mass of the tagged particle is fixed, so the translation diffusion constant is essentially zero and the shear viscosity of the Boltzmann lattice gas does indeed remain finite at zero frequency. Thus one would expect Eq. (5) to be valid with D set to zero.

The reason why this prediction differs from those given in Refs. 20 and 21 is that we have considered the long-time behavior of the AVACF for a particle with a nonzero rotational mobility. Had one instead considered a nonrotating particle, then the nonisotropic components of the bilinear variables would not get rapidly damped out at long times and they would contribute to the long-time tail coefficient. For an anisotropic Brownian particle, this is essentially the assumption made in Refs. 20 and 21, one does obtain a shape dependent coefficient. We stress again, though, that this shape dependence goes away if the particle is permitted to rotate.

III. DESCRIPTION OF THE MODEL

The system that we have used consists of a single colloidal particle suspended in a fluid, which is represented by a lattice gas simulated at the Boltzmann level. Extensive calculations of long-time correlations of the linear VACF of colloidal particles¹⁸ have been reported in which a lattice-gas cellular automaton model was used to represent the fluid. The lattice Boltzmann model is a preaveraged version of a lattice-gas cellular automaton (LGCA) model of a fluid. In lattice-gas cellular automaton the state of the fluid at any (discrete) time is specified by the number of particles at every lattice site and their velocity. Particles can only move in a limited number of directions (towards neighboring lattice points) and there can be at most one particle moving on a given “link.” The time evolution of the LGCA consists of two steps: propagation, during which every particle moves one time step, along its link to the next lattice site, and collision, where at every lattice site particles can change their velocities by collision (subject to the condition that these collisions conserve number of particles and momentum and retain the full symmetry of the lattice). In the lattice Boltzmann method (see, e.g., Ref. 22) the state of the fluid system is no longer characterized by the number of particles that move in direction \mathbf{c}_i on lattice site \mathbf{r} , but by the *probability* of finding such a particle. The single-particle distribution function $n_i(\mathbf{r}, t)$ describes the average number of particles at a particular node of the lattice \mathbf{r} , at a time t , with the discrete velocity \mathbf{c}_i . The hydrodynamic fields, mass density ρ , momentum density \mathbf{j} , and the momentum flux density $\mathbf{\Pi}$ are simply moments of this velocity distribution:

$$\rho = \sum_i n_i, \quad \mathbf{j} = \sum_i n_i \mathbf{c}_i, \quad \mathbf{\Pi} = \sum_i n_i \mathbf{c}_i \mathbf{c}_i. \quad (6)$$

The lattice model used in this work is the four-dimensional (4D) face-centered hypercubic (FCHC) lattice. A two- or three-dimensional model can then be obtained by projection

in the number of required dimensions. This FCHC model is used because three-dimensional cubic lattices do not have a high enough symmetry to ensure that the hydrodynamic transport coefficients are isotropic.

The time evolution of the distribution functions n_i is described by the discretized analog of the Boltzmann equation²³

$$n_i(\mathbf{r} + \mathbf{c}_i, t + 1) = n_i(\mathbf{r}, t) + \Delta_i(\mathbf{r}, t), \quad (7)$$

where Δ_i is the change in n_i due to instantaneous molecular collisions at the lattice nodes. The postcollision distribution $n_i + \Delta_i$ is propagated in the direction of the velocity vector \mathbf{c}_i . A complete description of the collision process is given in Ref. 24. The main effect of the collision operator $\Delta_i(\mathbf{r}, t)$ is to (partially) relax the shear stress at every lattice site. The rate of stress relaxation, or equivalently, the kinematic viscosity ν , can be chosen freely.

Simulating the lattice gas at the Boltzmann level has a number of advantages over the LGCA approach. The lattice Boltzmann model is purely dissipative, i.e., microscopic fluctuations in the fluid are not included (fluctuations can be incorporated in the lattice Boltzmann model by adding a suitable random noise term to the stress,⁹ but for the present work such fluctuations are not essential). In addition, some physically unrealistic properties of a lattice gas, such as a velocity dependent equation of state, can be eliminated. This approach—studying the motion of a single colloidal particle suspended in a lattice Boltzmann fluid—was used by Ladd⁹ to study the linear and rotational velocity autocorrelation functions of a sphere. The model we use differs in two respects. Firstly we employ a somewhat different method of integrating the equations of motion of the colloidal particle and second we consider nonspherical objects.

The motion of the colloidal particle is determined by the force and torque exerted on it by the fluid. These are in turn a result of the stick boundary conditions applied at the solid/fluid interface. For a stationary boundary a simple bounce-back rule performed on boundary links enforces the stick boundary condition. Boundary links are links connecting lattice sites inside and outside the solid object and obviously these come in pairs. We adopt a convention of labeling the link which goes from inside to outside as ib and its partner $-ib$. Stick boundary conditions with a moving boundary can be performed using the Boltzmann analog²⁴ of a scheme originally used for lattice gases.²⁵ For a moving boundary the bounce back rule is still applied but some of the particles moving in the same direction as the solid object are allowed to “leak” through, thus matching the fluid velocity to the object velocity at the boundary. For the lattice Boltzmann model the modified bounce-back rule takes the form

$$\begin{aligned} n_{-ib}(\mathbf{r}_b) &= n_{ib}(\mathbf{r}_b) - 4n_0(\rho)\mathbf{u}_b \cdot \mathbf{c}_{ib}, \\ n_{ib}(\mathbf{r}_b) &= n_{-ib}(\mathbf{r}_b) + 4n_0(\rho)\mathbf{u}_b \cdot \mathbf{c}_{ib}, \end{aligned} \quad (8)$$

where $n_0(\rho)$ is the zero velocity distribution and \mathbf{u}_b is the local boundary velocity. For a colloidal particle with linear and angular velocities of \mathbf{u}_0 and ω_0 , respectively, the local boundary velocity is just

$$\mathbf{u}_b = \mathbf{u}_0(t) + \omega_0(t) \wedge \mathbf{r}_b, \quad (9)$$

where \mathbf{r}_b is the vector connecting the center of mass of the object to the midpoint of the boundary link. The force \mathbf{F} and torque \mathbf{T} exerted by the fluid on the particle are computed from the change in momentum of the fluid resulting from the boundary collisions. The force at each individual boundary link, $\mathbf{F}_{ib}(\mathbf{r}_b)$ is given by

$$\mathbf{F}_{ib}(\mathbf{r}_b) = 2[n_{ib}(\mathbf{r}_b) - n_{-ib}(\mathbf{r}_b) - 4n_0(\rho)\mathbf{u}_b \cdot \mathbf{c}_{ib}]\mathbf{c}_{ib}. \quad (10)$$

The total force and torque acting on the object are calculated by summing these link forces, giving

$$\mathbf{F} = \sum_{ib} \mathbf{F}_{ib}(\mathbf{r}_b), \quad \mathbf{T} = \sum_{ib} \mathbf{F}_{ib}(\mathbf{r}_b) \wedge \mathbf{r}_b. \quad (11)$$

Taking the simplest discretized form of the equations of motion we have

$$\begin{aligned} \mathbf{u}'_0 &= \mathbf{u}_0(t + 1) = \mathbf{u}_0(t) + \mathbf{F}/m_0, \\ \omega'_0 &= \omega_0(t + 1) = \omega_0(t) + \mathbf{T}/I_0, \end{aligned} \quad (12)$$

where m_0 and I_0 are the mass and moment of inertia of the particle, respectively, and we have assigned a time step of unity. Equations (9)–(12) now define one possible method for updating the particle velocities.²⁴ Using this scheme the boundary collisions match the velocity of the fluid at the boundary to the old velocity of the particle, rather than the new velocity. In effect the fluid and boundary velocities are never the same. As a result \mathbf{u}_0 and ω_0 must change by only a small amount over one time step. In practice, this means that the density of the colloidal particle must be several times that of the fluid if stability is to be maintained.²⁴ An alternative is to rewrite Eq. (9) in terms of the new object velocities so that

$$\mathbf{u}_b = \mathbf{u}'_0 + \omega'_0 \wedge \mathbf{r}_b, \quad (13)$$

then substitute the modified expression for \mathbf{u}_b in Eqs. (10)–(12). Solving the resulting equations for the α component of \mathbf{u}'_0 and ω'_0 we find that

$$u'_{0\alpha} = \frac{m_0 u_{0\alpha}(t) + 2 \sum_{ib} [n_{ib}(\mathbf{r}_b) - n_{-ib}(\mathbf{r}_b)] c_{ib\alpha}}{m_0 + 8n_0(\rho) \sum_{ib} c_{ib\alpha} c_{ib\alpha}}, \quad (14)$$

$$\omega'_{0\alpha} = \frac{I_0 \omega_{0\alpha} + 2 \sum_{ib} [n_{ib}(\mathbf{r}_b) - n_{-ib}(\mathbf{r}_b)] (\mathbf{r}_b \wedge \mathbf{c}_{ib})_\alpha}{I_0 + 8n_0(\rho) \sum_{ib} (\mathbf{r}_b \wedge \mathbf{c}_{ib})_\alpha (\mathbf{r}_b \wedge \mathbf{c}_{ib})_\alpha}. \quad (15)$$

Using this rule the new fluid velocity at the boundary implies a force and torque on the object which, when incorporated into the equations of motion of the object, imply the same new velocity for the particle—the rule is self-consistent. Using this method we have found it possible to choose the density ratio freely.

To simulate a nonspherical particle we adopt the simplest conceivable approximation. We keep track of the position of the “true” boundary, in continuous space and, as the particle moves, we continuously update the list of boundary links on the basis of which nodes lie within this true boundary. The *exact* geometry of the particle, as represented on the lattice, depends on the orientation—although we always have an approximate representation of the object that we are

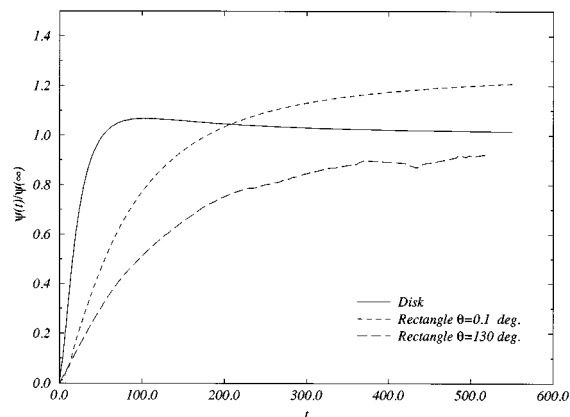


FIG. 1. The angular velocity autocorrelation function $\psi(t)$ in two dimensions. $\psi(t)$ has been normalized by the theoretical long-time result $\psi(\infty)$ given in the text. The solid line is the result for the disk, the narrow dashed line the result for a rectangle undergoing an angular displacement of 0.1° , and the broad dashed line the result for a rectangle undergoing an angular displacement of 130° .

nominally studying. If the long-time decay is independent of shape one may expect that these variations in the true geometry will be irrelevant anyway.

IV. RESULTS

We calculated the angular velocity autocorrelation function by applying an impulsive angular velocity, $\psi(0)$, to a colloidal particle in a stationary lattice Boltzmann fluid and correlating the rotational velocity at later times with the initial velocity. In all cases the viscosity ν of the fluid was equal to $\frac{1}{6}$ and the density ρ was 24 (all quantities are given in lattice units, where the mass of the lattice-gas particles, the lattice spacing and the time step are all unity). We performed the calculation for a spherical (or, in two dimensions, circular) particle, for a nonspherical object with a small initial velocity (so that the total angular displacement θ during a run was negligible), and for a nonspherical object with a large initial velocity (sufficient for the particle to undergo significant rotation during a run). In all cases, the maximum time up to which we calculated the AVACF was equal to the time taken for *any* information to cross the periodic box, so the effects of the periodic boundary conditions are completely eliminated.

In two dimensions the objects we used were a disc of radius 2.5 and a rectangle of width 3 and length 11. The moments of inertia were assigned to be 1632 and 8448, respectively. In both cases this corresponds approximately to a neutrally buoyant particle. For such a “light” particle the short-time exponential decay of the AVACF is quite rapid and the algebraic long-time decay is observable at shorter times. In Fig. 1 we plot the AVACF divided by the theoretically predicted long-time decay, $\psi(\infty)$. If the simulation reproduces the theoretical result we expect this function to asymptotically approach unity. Visually, the curve we obtain for the disk appears to be approaching unity. We can attempt to extrapolate to infinite times by plotting $\psi(t)/\psi(\infty)$ against $1/t$ and fitting a polynomial to the resulting function (this is

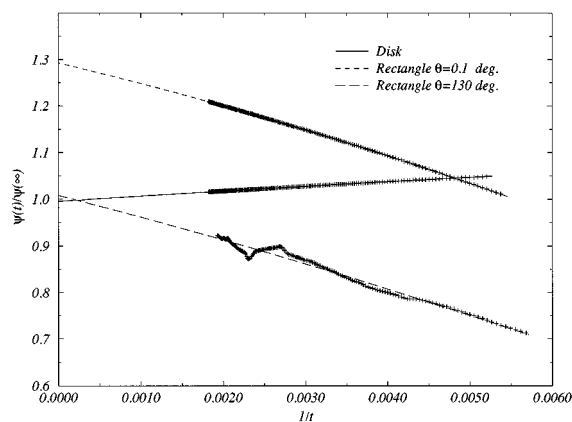


FIG. 2. Least-squares fits (the lines) to the function $\psi(t)/\psi(\infty)$ vs $1/t$ (the crosses) for the AVACF in two dimensions. The solid line is the fit for the disk, the narrow dashed line the fit for a rectangle undergoing an angular displacement of 0.1° , and the broad dashed line the fit for a rectangle undergoing an angular displacement of 130° .

shown in Fig. 2). By following this procedure we obtain a value $\psi(t \rightarrow \infty)/\psi(\infty) = 0.997 \pm 0.005$, so the agreement is quite satisfactory. It is worth pointing out that the moment of inertia we used in calculating $\psi(\infty)$ was the moment of inertia we assigned to the object. In the past the moment of inertia of the object was taken to be the assigned moment of inertia plus the moment of inertia of an equivalent volume of fluid inside the object.¹⁸ The argument was, that the fluid present inside the object (which is a necessary consequence of the way the boundary conditions are applied) contributed to an effective moment of inertia. Probably as a result of the modified rule we have used for updating the particle velocity, this does not seem to be the case in our work. The internal fluid has no effect and the effective moment of inertia is precisely the moment of inertia we assign.

The two curves plotted in Fig. 1 for the rectangular object correspond to angular displacements $\theta = 0.1^\circ$ and $\theta = 130^\circ$ over 500 time steps. What is clear from Fig. 1 is that the AVACF for the slowly rotating object *appears* to be approaching an asymptote which is not unity. Extrapolating to infinite times we find a value $\psi(t \rightarrow \infty)/\psi(\infty) = 1.31 \pm 0.01$, so the tail coefficient *does* appear to depend on the shape of the object *if* the angular displacement of the object is negligible. For the faster rotating rectangle the first thing to note is that although it is possible to see wobbles in the AVACF (a result of the discrete jumps in the representation of the object as it rotates) the dynamics are still plausible. The function is approaching an asymptote (so the algebraic form of the decay is correct) and what is more this asymptote appears to be close to unity. Extrapolating to infinite times we find an asymptotic value $\psi(t \rightarrow \infty)/\psi(\infty) = 1.02 \pm 0.05$. Therefore, once the angular displacement is significant (which in the real world would of course always be the case eventually) the tail coefficient in two dimensions is indeed *independent* of particle shape.

In three dimensions the objects we used were a sphere of radius 2.5 and a cylinder of diameter 3 and length 11, rotating in a plane parallel to its axis. The moments of inertia

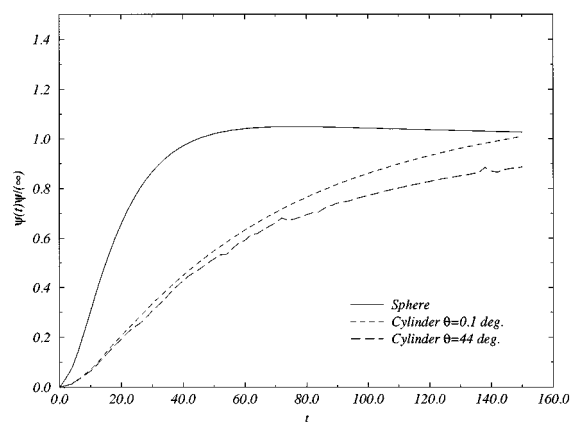


FIG. 3. The angular velocity autocorrelation function $\psi(t)$ in three dimensions. $\psi(t)$ has been normalized by the theoretical long-time result $\psi(\infty)$ given in the text. The solid line is the result for the sphere, the narrow dashed line the result for a cylinder undergoing an angular displacement of 0.1° , and the broad dashed line the result for a cylinder undergoing an angular displacement of 44° .

were assigned to be 5472 and 25344, respectively, again corresponding to roughly neutral buoyancy. The results we obtained for the AVACF, divided by the theoretical result for the long-time decay $\psi(\infty)$ are plotted in Fig. 3. Visually the curve for the sphere appears to be approaching unity. Following the same extrapolation procedure that we adopted in two dimensions we get a value $\psi(t \rightarrow \infty)/\psi(\infty) = 0.992 \pm 0.01$ (the extrapolation is shown in Fig. 4), so the agreement between theory and simulation is again satisfactory. The results for the cylinder tell the same story as the results for the rectangle in two dimensions. The slowly rotating cylinder, which only undergoes an angular displacement of 0.1° appears to be approaching an asymptote which is not unity. Extrapolating to infinite times we find a value $\psi(t \rightarrow \infty)/\psi(\infty) = 1.35 \pm 0.05$. However, for the faster rotating cylinder, which undergoes an angular displacement of 44° , the AVACF decays more rapidly at long times. Extrapolating to infinite

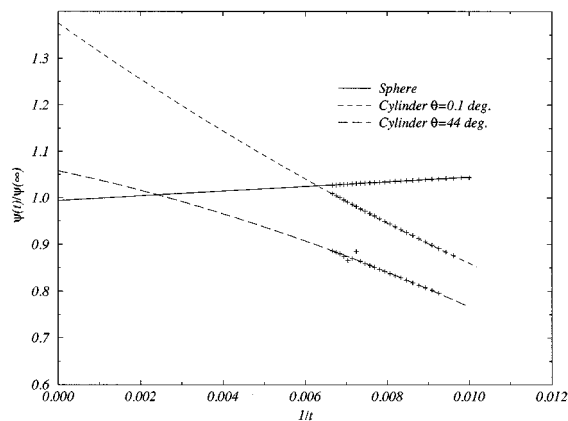


FIG. 4. Least-squares fits (the lines) to the function $\psi(t)/\psi(\infty)$ vs $1/t$ (the crosses) for the AVACF in three dimensions. The solid line is the fit for the sphere, the narrow dashed line the fit for a cylinder undergoing an angular displacement of 0.1° , and the broad dashed line the fit for a cylinder undergoing an angular displacement of 44° .

times we obtain a value $\psi(t \rightarrow \infty)/\psi(\infty) = 1.06 \pm 0.08$, which strongly suggests that in three dimensions, just as in two dimensions, the asymptotic decay of the AVACF is independent of particle shape once the particle has undergone significant rotation.

V. CONCLUSIONS

We outlined the derivation for the long-time decay of the angular velocity autocorrelation function in two dimensions. This theoretical result was in agreement with the results of a computer simulation in which we studied a rotating colloidal disk. In our simulations we were also able to reproduce the theoretical result for the decay of the AVACF of a sphere. A modification of the method used to update the particle velocities enabled us to study a neutrally buoyant particle which in turn made it easier to see the algebraic long-time decay. When we studied the long-time decay of the AVACF for a rectangle in two dimensions and a cylinder in three dimensions we found the same asymptotic decay as for the disk and cylinder, respectively, but only if the particle underwent significant rotation. If the particle remained essentially fixed then we saw an apparent shape dependent decay. These observations are also in agreement with theoretical predictions.

ACKNOWLEDGMENTS

The work of the FOM Institute is part of the scientific program of FOM and is supported by the Nederlandse Organisatie voor Wetenschappelijk Onderzoek (NWO). Computer time on the CRAY-C98/4256 at SARA was made available by the Stichting Nationale Computer Faciliteiten (Foundation for National Computing Facilities). We would like to thank Professor Felderhof for sending us a preprint of Ref. 22. Thanks also to Martin van der Hoef for access to his results and to Maarten Hagen and Bela Mulder for their critical reading of the manuscript.

- ¹ B. J. Alder and T. E. Wainwright, Phys. Rev. A **1**, 18 (1970).
- ² M. H. Ernst, E. H. Hauge, and J. M. J. van Leeuwen, Phys. Rev. Lett. **25**, 1254 (1970).
- ³ J. R. Dorfman and E. G. D. Cohen, Phys. Rev. Lett. **25**, 1257 (1970).
- ⁴ Y. W. Kim and J. E. Matta, Phys. Rev. Lett. **31**, 208 (1973).
- ⁵ P. D. Fedele and Y. W. Kim, Phys. Rev. Lett. **44**, 691 (1980).
- ⁶ G. L. Paul and P. N. Pusey, J. Phys. A **14**, 3301 (1981).
- ⁷ Chr. Morkel, Chr. Gronemeyer, W. Gläser, and J. Bosse, Phys. Rev. Lett. **58**, 1873 (1987).
- ⁸ M. A. van der Hoef and D. Frenkel, Phys. Rev. A **41**, 4277 (1990).
- ⁹ A. J. C. Ladd, Phys. Rev. Lett. **70**, 1339 (1993).
- ¹⁰ M. Hagen, C. P. Lowe, and D. Frenkel, Phys. Rev. E (to be published).
- ¹¹ N. K. Ailawadi and B. J. Berne, J. Chem. Phys. **54**, 3569 (1971).
- ¹² N. K. Ailawadi and S. Harris, J. Chem. Phys. **56**, 5783 (1972).
- ¹³ E. H. Hauge and A. Martin-Löf, J. Stat. Phys. **7**, 259 (1973).
- ¹⁴ T. S. Chow, Phys. Fluids **16**, 31 (1973).
- ¹⁵ A. J. Masters and T. Keyes, J. Stat. Phys. **39**, 215 (1985).
- ¹⁶ G. Subramanian, D. G. Levitt, and H. T. Davis, J. Stat. Phys. **15**, 1 (1976).
- ¹⁷ M. A. van der Hoef, D. Frenkel, and A. J. C. Ladd, Phys. Rev. Lett. **67**, 3459 (1991).
- ¹⁸ M. A. van der Hoef, Ph.D. thesis, University of Utrecht, 1992.
- ¹⁹ F. Garisto and R. Kapral, Phys. Rev. A **13**, 1652 (1976).
- ²⁰ R. Hocquart and E. J. Hinch, J. Fluid Mech. **137**, 217 (1983).

²¹B. Cichocki and B. U. Felderhof, *Physica A* **213**, 465 (1995).

²²G. R. McNamara and B. J. Alder, in *Microscopic Simulation of Complex Hydrodynamic Phenomena*, edited by M. Mareschal and B. L. Holian (Plenum, New York, 1992).

²³U. Frisch, D. d'Humières, B. Hasslacher, P. Lallemand, Y. Pomeau, and J.-P. Rivet, *Complex Syst.* **1**, 649 (1987).

²⁴A. J. C. Ladd, *J. Fluid Mech.* **271**, 285 (1994).

²⁵A. J. C. Ladd and D. Frenkel, *Phys. Fluids A* **2**, 1921 (1990).